Relationship Between Crystal Symmetry and Magnetic Properties of Ionic Compounds Containing Mn^{3+}

J. B. GOODENOUGH, A. WOLD, R. J. ARNOTT, AND N. MENYUK
Lincoln Laboratory, Massachusetts Institute of Technology, Lexington, Massachusetts*
(Received January 30, 1961; revised manuscript received July 3, 1961)

An investigation has been made of the relationship between crystallographic symmetry and $Mn^{3+}-O^{2-}-Mn^{3+}$ 180° superexchange interactions in several perovskite systems. In particular, crystallographic and magnetic measurements have been made on a number of samples in the systems $La(Mn_{1-x}M_x)O_{3+\delta}$, where $M=$Ga, Co, Ni. In all three systems, the $Mn^{3+}-O^{2-}-Mn^{3+}$ interactions are found to be ferromagnetic for *O*-orthorhombic samples having $a<c/\sqrt{2}<b$. For $x<0.5$ in the system $M=$Ga, there is *O'*-orthorhombic symmetry ($c/\sqrt{2}<a<b$) and ferrimagnetism that is suggestive of anisotropic $Mn^{3+}-O^{2-}-Mn^{3+}$ interactions, similar to those found in $LaMnO_3$, and preferential ordering of the Ga^{3+} into one magnetic sublattice. Measurements of Curie temperature vs composition in this system support ordering of the gallium in the compositional range $x\leq 0.4$, partial ordering in the range $0.4<x\leq 0.6$. These observations are consistent with the magnetic measurements of various other workers on the systems $(La,M'^{2+})MnO_{3+\delta}$, $La(Mn,Cr)O_3$ $(La,Ba)(Mn,Ti)O_3$.

The ferromagnetic $Mn^{3+}-$anion$-Mn^{3+}$ interactions that occur in the perovskites with *O*-orthorhombic or rhombohedral symmetry and in the NiAs-type compounds cannot be accounted for by present superexchange theory if the electron configuration about a Mn^{3+} ion is assumed fixed with one electron arithmetically averaged over the two e_g orbitals, or if static, local distortions are randomly distributed through the structure. It is pointed out that Jahn-Teller electronic ordering is fast relative to the atomic vibrations so that there is strong coupling of the vibrational modes and the e_g-electron configuration. This means that the electron configuration that is used in the superexchange calculation must be correlated with the vibrational modes. If this is done, a ferromagnetic $Mn^{3+}-$anion$-Mn^{3+}$ interaction follows from the superexchange theory.

I. INTRODUCTION

A NUMBER of samples of the perovskite systems $La(Mn_{1-x}M_x)O_{3+\delta}$, where $M=$Ga, Co, and Ni have been prepared and several crystallographic and magnetic properties have been measured. It is found that the nature of the $Mn^{3+}-O^{2-}-Mn^{3+}$ 180° superexchange interactions are structure-dependent. Samples with *O'*-orthorhombic symmetry ($c/\sqrt{2}<a\leq b$) have Mn^{3+}-occupied octahedral interstices with relatively large distortions from cubic symmetry which reflect electronic ordering about the Mn^{3+} cations, whereas those with *O*-orthorhombic symmetry ($a<c/\sqrt{2}<b$) do not. Samples with *O'*-orthorhombic symmetry have anisotropic $Mn^{3+}-O^{2-}-Mn^{3+}$ superexchange: Within a (001) plane the coupling is ferromagnetic and between planes it is antiferromagnetic. The *O*-orthorhombic samples on the other hand, have isotropic ferromagnetic $Mn^{3+}-O^{2-}-Mn^{3+}$ interactions.[1] The details of the sample preparation and purity as well as the experimental techniques and findings are presented in Sec. II.

In order to apply superexchange theory to obtain a set of rules for magnetic coupling between various cations, it is necessary to have a detailed knowledge of the static and dynamic relationships of the crystalline fields and the outer-electron configurations. These relationships are considered in Sec. III, where a "quasi-static" model for superexchange between Mn^{3+} ions in "undistorted" octahedra is presented. This model is shown to be consistent with existing theories for superexchange and to enable extension of the rules for the sign of the 180° superexchange interactions to include the various possibilities for Jahn-Teller ions in different types of environments.

In Sec. IV the theoretical model is applied to the experimental data. It is found that the anisotropic coupling that occurs in *O'*-orthorhombic samples follows from a straightforward application of existing theory, since here the pertinent electron configurations are static and have been adequately defined. The isotropic, ferromagnetic coupling that occurs in *O*-orthorhombic samples is shown to follow from the fact that the lattice vibrations are capable of correlating the electron configurations of neighboring cations. The addition of this correlation effect permits a straightforward interpretation of all the various 180° superexchange interactions that have been observed. It is further shown that the magnetic measurements permit this model for the electron configurations to be selected in preference to other alternatives that have been proposed.

Finally, it is pointed out that the present model provides a possible mechanism for the interpretation of the magnetic coupling that has been observed in NiAs-type compounds.

II. EXPERIMENTAL

A. Chemical Preparation

1. $La(Mn_{1-x}Ga_x)O_3$

Spectroscopic-grade lanthanum oxide and gallium oxide were ignited at 800°C for three hours to insure complete decomposition of carbonates and removal of water. These oxides were then cooled over a phosphorous pentoxide desiccant and weighed amounts were intimately mixed with Mn_2O_3. After several hours of thorough grinding, the mixture was pressed into $\frac{1}{4}$-in. pellets and placed in a platinum crucible. The crucible was sealed in an evacuated, heavy-walled silica tube. It

* Operated with support from the U. S. Army, Navy, and Air Force.

[1] For a complete discussion of the *O* and *O'* orthorhombic symmetry as well as a summary of the available experimental data on perovskites, see J. B. Goodenough, *Landolt-Bornstein Tabellen* [Springer-Verlag, Berlin (to be published)].

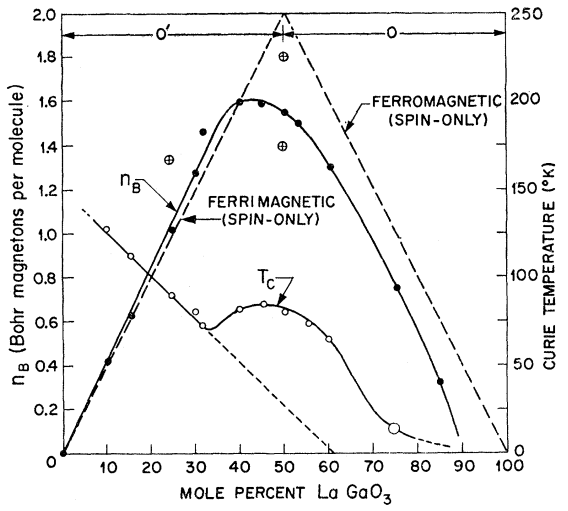

FIG. 1. Saturation magnetization and Curie temperature for the system $La(Mn_{1-x}Ga_x)O_3$. The points ⊕ are Curie temperatures for $La(Mn_{0.75}Co_{0.25})O_3$ and $La(Mn_{0.5}Co_{0.5})O_3$. The double Curie temperature of the latter composition reflects two magnetic phases found in a single sample.

is important that the samples be first fired at 800°C for two days in order to minimize any attack of the silica capsule. The sample was subsequently fired for twenty-four hours at 900°, 1000°, and twice at 1100°C, the sample being reground before each of the four firings. The product was ground, sifted through a 325-mesh screen, and analyzed by both chemical and x-ray techniques. The valence state of manganese was confirmed by standard chemical procedures. In all samples the manganese was present as Mn^{3+} with less than 1% Mn^{2+}. There was no evidence of Mn^{4+} in any of the samples.

2. $La(Mn_{1-x}Co_x)O_{3+\delta}$

Compositions in the system $La(Mn_{1-x}Co_x)O_{3+\delta}$ were prepared by heating mixtures of La_2O_3, Mn_2O_3, and $CoCO_3$ to 1300°C. At 1300°C, it was not possible to heat the samples in evacuated silica capsules. The samples were heated in air and the products were analyzed for total oxidizing or reducing power, the analysis being compared with values expected for the $Mn^{3+}-Co^{3+}$ compound. In the compositional range $0.4 \leq x \leq 0.6$, a two-phase region appeared at 1300°C; one was rhombohedral, like $LaCoO_3$ and the other was orthorhombic (O, not O'). In addition two samples, $x=0.25$ and 0.5, were prepared at 1100°C *in vacuo* for Curie-point determinations. These samples contained no Mn^{4+} and the x-ray patterns, though too poor for measurements, indicated two phases in the sample $x=0.5$.

3. $La(Mn_{1-x}Ni_x)O_{3+\delta'}$

Samples of $La(Mn_{1-x}Ni_x)O_{3+\delta'}$ were prepared by reacting La_2O_3 with varying molar mixtures of NiO and Mn_2O_3 in air at 1100°C. The products were annealed at 800°C in vacuum to improve their crystallinity. These materials were made as part of an earlier investigation[2] and therefore were not prepared *in vacuo*, as was the gallium series.

B. Measurements

1. Magnetization

The magnetization measurements, which were made with a vibrating-coil magnetometer,[3] were taken at 4.2°K in magnetic fields of approximately 6, 9, and 11 koe. The saturation magnetization was then determined by extrapolating the measured moment to infinite field.

The resulting saturation magnetizations for the system $La(Mn_{1-x}Ga_x)O_3$ are given in Fig. 1. For $x<0.5$, the magnetization closely follows the dashed line labeled *ferrimagnetic*. This line was obtained by assuming that each diamagnetic Ga^{3+} ion orders on the same magnetic sublattice and that each Mn^{3+} ion carries a spin-only moment of $4\mu_B$. For $x>0.5$, the magnetization approaches that for ferromagnetic alignment of all the Mn^{3+} moments.

A similar set of measurements for samples of the system $La(Mn_{1-x}Co_x)O_{3+\delta}$ revealed strikingly different magnetic properties, as shown in Fig. 2, even though the cobalt ions presumably exist as low-spin-state (diamagnetic) Co^{III}. It is particularly noteworthy that in the region $0.25 \leq x \leq 0.5$ the magnetization is approximately

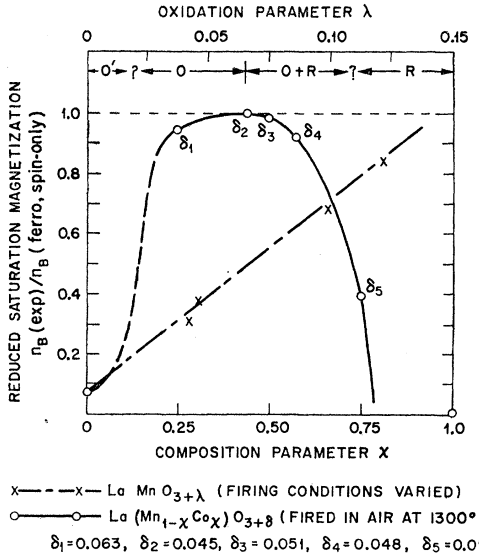

FIG. 2. Reduced saturation magnetization at 4.2°K, with spin-only ferromagnetism the reference magnetization, for the systems $La(Mn_{1-x}Co_x)O_{3+\delta}$ and $LaMnO_{3+\lambda}$. Trivalent cobalt is assumed diamagnetic. End members stoichiometric. Crystallographic phases, O=orthorhombic and R=rhombohedral, refer to $La(Mn_{1-x}Co_x)O_{3+\delta}$.

[2] A. Wold, R. J. Arnott, and J. B. Goodenough, J. Appl. Phys. **29**, 387 (1958).

[3] K. Dwight, N. Menyuk, and D. O. Smith, J. Appl. Phys. **29**, 491 (1958).

$4\mu_B$ per Mn^{3+} ion plus $3\mu_B$ per Mn^{4+} ion, indicating ferromagnetic $Mn^{3+}-O^{2-}-Mn^{3+}$ and $Mn^{3+}-O^{2-}-Mn^{4+}$ interactions. By contrast, compositions of $La(Mn_{1-x}Ga_x)O_3$ in this range are ferrimagnetic, indicating anisotropic $Mn^{3+}-O^{2-}-Mn^{3+}$ interactions that are ferromagnetic in some directions, antiferromagnetic in others. The number of Mn^{4+} ions present in the cobalt-substituted system is not sufficient to account for the discrepancy, as can be estimated from the data for $LaMnO_{3+\lambda}$ that are also plotted in Fig. 2.

Magnetization measurements for samples of $La(Mn_{1-x}Ni_x)O_{3+\delta'}$ also indicate (see Fig. 3) ferromagnetic $Mn^{3+}-O^{2-}-Mn^{3+}$ interactions throughout the range $0.25 \leq x \leq 0.5$, the net magnetization corresponding to ferromagnetic alignment of $4\mu_B$ per Mn^{3+}, $3\mu_B$ per Mn^{4+}, and $1\mu_B$ per Ni^{III}. Again the fraction of Mn^{4+} present is not sufficient to account for the ferromagnetic coupling.

2. *Curie Temperature*

Curie-point determinations were made for each sample of the $La(Mn_{1-x}Ga_x)O_3$ system. The samples were cooled to 4.2°K in a field of 10 koe; the field was then reduced to 700 oe and the sample slowly warmed through the Curie temperature. The Curie point was taken as the intersection of the magnetization axis by the tangent to the magnetization curve at its point of steepest slope. The resultant values are given in Fig. 1. The magnetization curves of the samples containing 50, 55 and 68% manganese had tangents with relatively steep slopes; the curves of the other samples had relatively small slopes. The small slope is indicative of some compositional variation within the sample and leads to a Curie-temperature reading that is higher than the true

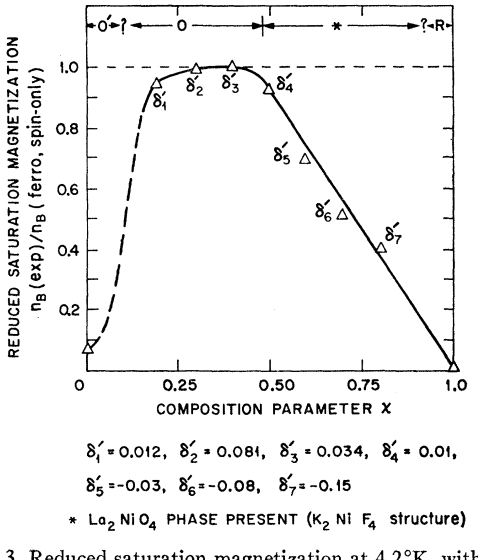

FIG. 3. Reduced saturation magnetization at 4.2°K, with spin-only ferromagnetism the reference magnetization, for the system $La(Mn_{1-x}Ni_x)O_{3+\delta'}$ fired in air at 1100°C and annealed at 800°C. Trivalent nickel is assumed to carry one Bohr magneton (low-spin-state). End members stoichiometric.

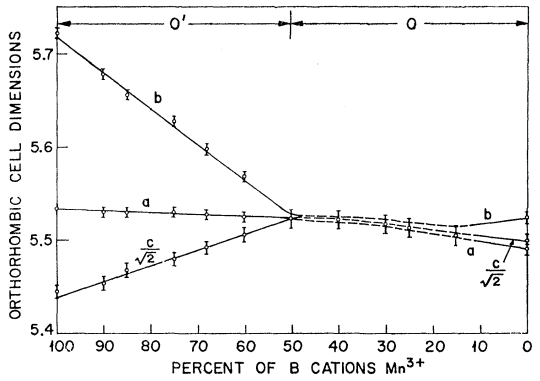

FIG. 4. Variation of lattice parameters with composition in the system $La(Mn_{1-x}Ga_x)O_3$.

value for the nominal composition tested. The error due to this effect is estimated to be of the order of +3°C, and is additional to the measurement uncertainty of ±2°C. Substitution of gallium into $LaMnO_3$ causes a decrease in Curie temperature that is linear with the percentage of substitution up to approximately 30% gallium. Further gallium substitution causes an apparently anomalous rise in the Curie point, a maximum value occurring at 50% gallium. Beyond this composition, further gallium substitution produces a rapid decrease in the Curie temperature.

Similar Curie-point measurements were made of samples of $La(Mn_{0.5}Co_{0.5})O_3$ and $La(Mn_{0.75}Co_{0.25})O_3$ that were specially prepared to eliminate Mn^{4+} content. Since these samples were fired at 1100°C, they were probably incompletely reacted, so no absolute measurements of the magnetization were taken. The magnetization curve of $La(Mn_{0.5}Co_{0.5})O_3$ showed the presence of two distinct magnetic phases, with Curie points of 225°K and approximately 175°K. On the other hand, $La(Mn_{0.75}Co_{0.25})O_3$ had a single, well-defined Curie temperature of 168°K. These values are also shown in Fig. 1.

3. *X-Ray Analysis*

Room-temperature parameters for the system $La(Mn_{1-x}Ga_x)O_3$, obtained with FeK_α radiation and a Norelco diffractometer, are plotted in Fig. 4. All members were orthorhombic, but poorly crystallized. It is noted that the symmetry remains *O'* throughout the range $0 \leq x < 0.5$. The ratio $c/\sqrt{2}a$ is plotted in Fig. 5. The symmetry is *O'* for $c/\sqrt{2}a < 1$, and is *O* for $c/\sqrt{2}a > 1$. For samples in the range $0.5 \leq x \leq 0.85$, the combination of poor crystallinity and small distortions did not permit accurate resolution of the diffraction-pattern splittings. Therefore only a mean cubic parameter was calculated and plotted in Fig. 4 for each sample throughout this range, even though the pattern showed definite indications of small splitting indicative of the *O* symmetry. Examination[4] of $LaMnO_{3+\lambda}$, prepared under varied

[4] A. Wold and R. J. Arnott, J. Phys. Chem. Solids **9**, 176 (1959).

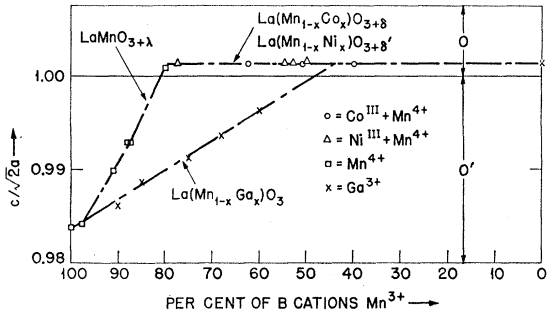

FIG. 5. Lattice-parameter ratio $c/\sqrt{2}a$ for orthorhombic perovskites in the systems $La(Mn_{1-x}{}^{3+}M_x)O_{3+y}$, where $M=Co^{III}+Mn^{4+}$, $Ni^{III}+Mn^{4+}$, and Ga^{3+}.

firing conditions, shows that the symmetry changes from O' to O at about 20% Mn^{4+}, or $\lambda=0.10$ (see Fig. 5). The most significant fact in Fig. 5, however, is the difference in symmetry in the range 80>percent $Mn^{3+}\geq 50$ for the system $La(Mn_{1-x}Ga_x)O_3$, on the one hand, and $La(Mn_{1-x}Co_x)O_{3+\delta}$, $La(Mn_{1-x}Ni_x)O_{3+\delta'}$, on the other. These crystalline symmetries suggest an electronic ordering in the system $La(Mn_{1-x}Ga_x)O_3$ that is similar to that found in pure $LaMnO_3$, but no long-range, cooperative Jahn-Teller distortions about Mn^{3+} ions in the samples of the other two systems that were studied. This suggestion is, of course, strengthened by the observation (see Figs. 1–3) of different magnetic interactions for the two classes of systems.

It was also noted that, in samples of the system $La(Mn_{1-x}Ni_x)O_{3+\delta'}$, a second phase ($La_2NiO_4$ with K_2NiF_4 structure) was present throughout the range $0.5\leq x\leq 0.8$. The end member, $LaNiO_3$, had rhombohedral symmetry. The system $La(Mn_{1-x}Co_x)O_{3+\delta}$ contained two phases, a rhombohedral and an O-orthorhombic perovskite, in the range $0.5\leq x\leq 0.6$. There were also indications of two phases in the $x=0.5$ sample prepared at 1100°C. The existence of two phases in this sample was also indicated by the double Curie point shown in Fig. 1. The end member, $LaCoO_3$, is rhombohedral.

III. THEORY

Rules for the sign of the 180° superexchange interaction between cation moments via an anion intermediary in an ionic crystal have been proposed[5,6] and given semiquantitative justification.[7–11] These rules, which are summarized later in Fig. 9 for octahedral-site cations, depend upon the number of d electrons and their configuration at the cations on either side of the anion intermediary. Therefore to properly apply these rules, it is necessary to know the electron configurations.

A. Electron Configurations

The d-electron configuration is primarily determined by the internal crystalline fields. The strongest crystalline fields at a cation are those due to the adjacent anions. In an octahedral interstice, the cation d levels are split as indicated in Fig. 6.[12] Here E_{ex} is the intra-atomic exchange splitting responsible for Hund's rule and Δ is the cubic-field splitting. Frequently the symmetry of the cation sublattice introduces trigonal fields that are superposed on the anion-sublattice field. The trigonal splittings are also indicated in Fig. 6. Such energy diagrams provide the essential information about electron configurations.

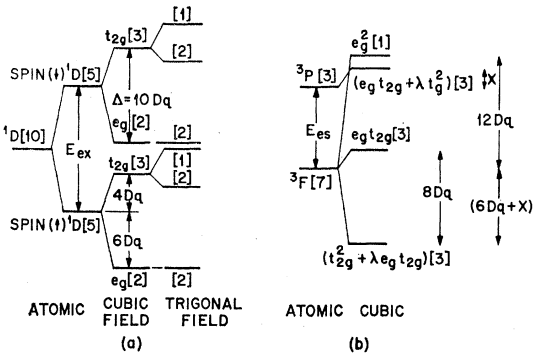

FIG. 6. Octahedral-site, crystal-field splittings for (a) one outer d hole corresponding to high-spin-state ($E_{ex}>\Delta$) $3d^4$ cation and (b) two or seven outer d electrons. For one outer d electron, $E_{ex}=0$ and the order of crystal-field splitting in (a) reversed. For six outer d electrons the order of crystal-field splittings in (a) is reversed. Similarly for two outer d holes corresponding to a d^3 or a d^8 cation, the order of the crystal-field splittings in (b) is reversed. Empirically, $\lambda\approx 0.1$ so that (a), with order of levels inverted, is an adequate one-electron model for qualitative arguments needed for the sign of the 180° superexchange interactions. The degeneracy of each level is indicated in brackets.

For the special case of $E_{ex}\gg\Delta=10Dq$ and four outer d electrons, which may occur if the outer-electron configuration is $3d^4$ (as in Mn^{3+}, Cr^{2+}), the problem is equivalent to that of a single hole. In this case, the orbital ground state for cubic symmetry is twofold-degenerate E_g, and the orbital angular momentum is largely quenched by the cubic-field splitting Δ. Jahn and Teller[13,14] have pointed out that in such a case a configuration of lower symmetry splits the orbital degeneracy into two nondegenerate levels, where the mean value of the two first-order energies is equal to the energy of the original degenerate level. This means that

[5] J. B. Goodenough, Phys. Rev. **100**, 564 (1955); J. Phys. Chem. Solids **6**, 287 (1958); J. phys. radium **20**, 155 (1959).
[6] J. Kanamori, J. Phys. Chem. Solids **10**, 87 (1959).
[7] R. K. Nesbet, Ann. Phys. **4**, 87 (1958); Phys. Rev. **119**, 658 (1960).
[8] P. W. Anderson, Phys. Rev. **115**, 2 (1959).
[9] J. Kondo, Progr. Theoret. Phys. (Kyoto) **22**, 41 (1959).
[10] F. Keffer and T. Oguchi, Phys. Rev. **115**, 1428 (1959).
[11] T. R. Waite, J. Chem. Phys. **33**, 256 (1960).
[12] The Mulliken nomenclature is used wherein the threefold-degenerate T_{2g} state (containing t_{2g} electrons or holes) is formed from d_{xy}, d_{yz}, d_{zx} orbitals and the twofold-degenerate E_g state (containing e_g electrons or holes) is formed from the d_{z^2} and $d_{x^2-y^2}$ orbitals.
[13] H. A. Jahn and E. Teller, Proc. Roy. Soc. (London) **A161**, 220 (1937).
[14] H. A. Jahn, Proc. Roy. Soc. (London) **A164**, 117 (1938).

the cubic symmetry is not stable; that is, the system has lower energy if the crystalline fields at the $3d^4$ cations are less symmetrical. The splittings of the E_g state by two types of tetragonal distortion are shown in Fig. 7. Significantly, it has been shown[15–17] that although the electronic state for a stable configuration of the nuclear framework is nondegenerate, the system has a vibrational degeneracy arising from the fact that there are two or more stable configurations that are geometrically equivalent, and therefore have the same energies. For example, the two tetragonal distortions of Fig. 7 are mirror images of one another. This type of distortion, which splits the $d_{x^2-y^2}$ and d_{z^2} orbitals, is referred to as mode Q_3. There is also a mode Q_2 that is congruent to Q_3; it consists of a movement of the anion nuclei along the [100] away from the center of symmetry and along the [010] toward the center of symmetry. In this case the split orbitals are a mixture of d_{z^2} and $d_{x^2-y^2}$. If polar coordinates ρ and θ in the space of the coordinates Q_2 and Q_3 are defined ($Q_3=\rho\cos\theta$, $Q_2=\rho\sin\theta$), then to first order in the coupling between modes Q_2, Q_3 and orbitals d_{z^2}, $d_{x^2-y^2}$, the ground-state energy for an isolated $Mn^{3+}(O^{2-})_6$ complex is independent of θ. This means that the ground state is not uniquely determined, but corresponds to any point on the circle with radius $\rho=\delta$, where δ is proportional to the coupling constant and the inverse root of the stiffness constant associated with the vibrations. A consequence of this is that the degeneracy may be removed by resonance between the stable configurations. The degeneracy may also be removed by the addition of anharmonic terms in the potential energy and higher-order coupling terms, which makes the total energy at $T=0°\text{K}$

$$E=-\delta^2\{\tfrac{1}{2}C+(A_3-B_3\delta)\cos3\theta\}, \qquad (1)$$

where A_3 is generally positive.[16] With a point-charge model, B_3 is calculated to be positive,[17] and the sign of the $\cos3\theta$ term is uncertain. However if covalency favors bond formation, as is probably the case, B_3 is negative and the stable state unambiguously favors $\cos3\theta=1$, or $\theta=0, \pm2\pi/3$. This corresponds to Q_3 ($c/a>1$) with c axis oriented along the z, x, and y axes, respectively. In the perovskite lattice, on the other hand, the lowest mode, given no anharmonicity, turns out to be $\pm Q_2$, the short (s) and long (l) axes alternating along the [100] and [010] axes of the pseudotetragonal cell.[18] Addition of the anharmonic terms bends the two vectors towards $\theta=\pm2\pi/3$. The extreme-anisotropy case ($\theta=\pm2\pi/3$) corresponds to an ordering of d_{z^2} orbitals as shown in Fig. 8. Thus the presence of higher-order coupling terms and of anharmonic terms in the vibrational energy may stabilize a static distortion of the interstices at low temperatures. In a solid with a large percentage of Jahn-Teller cations, these distortions are cooperative and therefore give rise to measurable changes in the crystalline symmetry. At higher temperatures entropy considerations can be expected to favor either (a) noncooperative static distortions or (b) removal of the degeneracy by resonance between the stable configurations. In Sec. IV it is shown that the experiments reported in this paper support the second alternative.

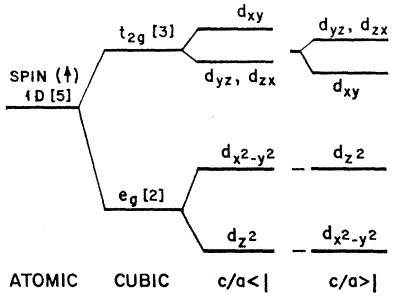

FIG. 7. Tetragonal-field splittings for one d hole corresponding to a $3d^4$ cation.

The dynamic problem, which represents a doubly degenerate electronic state E_g whose degeneracy is removed in first order by a doubly degenerate vibration, has been studied by several workers.[19–21] These studies, which were restricted to an isolated complex, indicate not only that the ground-state degeneracy is removed by coupling between the nuclear vibrations and the electron configuration, but also that for strong coupling the electrons are in a "Born-Oppenheimer" potential so that the electronic configuration "follows" the nuclear vibrations. Thus for sufficiently large coupling the electronic configuration corresponds to the symmetry of the nuclei, the nuclear motions being slow relative to the electronic motions. In this limit, then, the electronic configuration at any moment of time can be approxi-

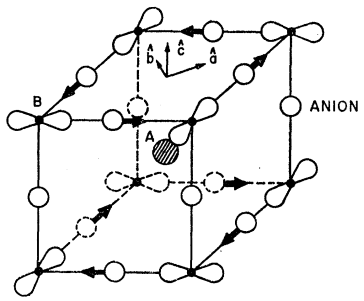

FIG. 8. Schematic diagram of ordering of the single e_g electron on the $3d^4$ B cations given O'-orthorhombic ($c/\sqrt{2}<a\leq b$) symmetry. This represents extreme anisotropy case. Zero anisotropy would also have electron density along c axis so that each c-axis cation-anion-cation interaction corresponded to Case 1 rather than Case 3 of Table I. The true situation lies somewhere between the two extremes.

[15] J. H. Van Vleck, J. Chem. Phys. **7**, 72 (1939).
[16] U. Opik and M. H. L. Pryce, Proc. Roy. Soc. (London) **A238**, 425 (1957).
[17] A. D. Liehr and C. Ballhausen, Ann. Phys. **3**, 304 (1958).
[18] J. Kanamori, Suppl. J. Appl. Phys. **31**, 14S (1960).
[19] H. C. Longuet-Higgins, U. Opik, M. H. L. Pryce, and R. A. Sack, Proc. Roy. Soc. (London) **A244**, 1 (1958).
[20] W. Moffitt and A. D. Liehr, Phys. Rev. **106**, 1195 (1957).
[21] W. Moffitt and W. Thorson, Phys. Rev. **108**, 1251 (1957).

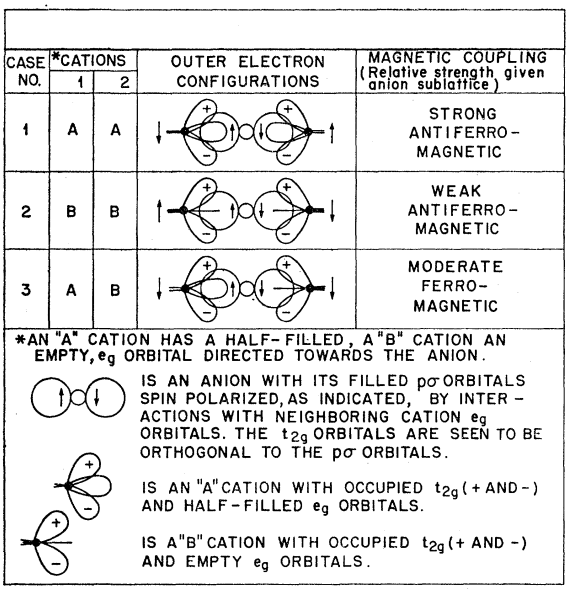

FIG. 9. Rules for 180° superexchange interactions.

mated by the "quasistatic" ground-state configuration associated with the nuclear positions at that moment. This limit will be referred to in this paper as the *quasistatic limit.*

B. Superexchange Theories

Several contributions to the superexchange interactions of the electron configurations represented by Fig. 9 have been identified and given analytic expression. In the 180° case, the important terms are additive and of the form of the Heisenberg exchange Hamiltonian

$$H=-\sum_{ij} J_{ij}\mathbf{S}_i\cdot\mathbf{S}_j. \qquad (2)$$

The three principal contributions have been referred to[22] as delocalization superexchange,[8,11] correlation superexchange,[7] and polarization superexchange.[9,10] The various mechanisms are briefly presented in the Appendix to establish the physical origins of the rules of Fig. 9. The various analytic expressions may be found in the literature references cited.

C. Superexchange between Jahn-Teller Cations: The Quasistatic Hypothesis

Application of the superexchange rules of Fig. 9 is straightforward once the outer-electron configuration at the cations is defined. As has been noted, most electron configurations follow directly from crystal-field theory, but in the case of Jahn-Teller ions special precautions must be taken. If there are cooperative, static Jahn-Teller distortions, it is possible to obtain the electron configurations at the Jahn-Teller ions from an experimental determination of the positions of the atomic nuclei in their neighborhood. This requires no new principle. If there are no cooperative, static Jahn-Teller distortions, it is necessary to make an assumption about the electron configurations. There are three possible assumptions that can be made: (a) There are static, local Jahn-Teller distortions, but these distortions are random, having no cooperative, long-range order. (b) There are no static, local distortions; but strong coupling to the nuclear vibrations removes the orbital degeneracy and correlates the electron spin configurations of neighboring Jahn-Teller ions. (c) There are no static, local distortions; and weak coupling to the nuclear vibrations, although it removes the orbital degeneracy, leaves the spin configurations of neighboring Jahn-Teller ions uncorrelated. Theoretical arguments for each of these alternatives are presented below, and in Sec. IV it is shown that the experimental data presented in this paper indicate alternative (b), the quasistatic hypothesis, is the correct alternative for $3d^4$ cations.

Wojtowicz[23] used assumption (a) in a statistical treatment of the order-disorder transition and of the temperature variation of the c/a ratio for spinels that are distorted by cooperative, Jahn-Teller electron ordering. With this model, he was able to obtain semiquantitative agreement with the experimental c/a ratios, and to correctly predict a first-order tetragonal $\rightleftharpoons$ cubic phase transformation for the spinels, a second-order $O'\rightleftharpoons O$ phase transformation for Jahn-Teller-distorted perovskites. Consistent with assumption (a), he also assumed high vibrational anisotropies, which removes the Q_2, Q_3 degeneracy. With such a model, the e_g electron-configuration about a Mn^{3+} ion is $(2z^2-x^2-y^2)$, $(2x^2-y^2-z^2)$ or $(2y^2-z^2-x^2)$ and the three alternatives are *randomly* distributed through the structure.

Kanamori[18] has also discussed the temperature variation of the c/a ratio in Jahn-Teller-distorted spinels. He assumed no static, local distortions in his analysis [assumption (b) or (c)]; and he also obtained semiquantitative agreement with the experimental c/a ratios, a first-order phase transformation in spinels, and a second-order transformation in perovskites. Consistent with his assumption he placed no restrictions on the ratio Q_2/Q_3 in his static, perovskite distortions and he required only small vibrational anharmonicity in the spinels.

Therefore it appears that measurements of crystallographic or thermodynamic variables are unable to distinguish between the three alternatives (a)–(c). However, the three models predict quite different electron configurations for the cubic or O-orthorhombic phases and therefore different magnetic coupling, so that discrimination between the three models can be obtained from magnetic measurements. This empirical discrimination is made in Sec. IV.

To obtain a theoretical estimate for discrimination between alternatives (b) and (c), it is reasonable to

[22] R. K. Nesbet, Phys. Rev. **122**, 1497 (1961).

[23] P. Wojtowicz, Phys. Rev. **116**, 32 (1959); Bull. Am. Phys. Soc. 4, 63 (1959).

assume that alternative (b) is preferred if

$$\nu_n \ll \Delta E_{JT}/h, \tag{3}$$

and alternative (c) if

$$\nu_n \gg \Delta E_{JT}/h, \tag{4}$$

where ν_n is the nuclear-vibration frequency, h is Planck's constant, and ΔE_{JT} is the Jahn-Teller stabilization associated with a deformation of the interstice to a reduced symmetry. These relationships follow from the Born-Oppenheimer[24] argument that the relatively small ratio of electron to nuclear masses makes possible electron motions that are rapid relative to any nuclear motions. This means that, if the driving energy for the electrons is large compared to $h\nu_n$, the electron configuration is able to follow the nuclear motions, in accordance with the quasistatic hypothesis. If the driving energy is small compared to $h\nu_n$, the electron configuration deviates little from that for orbital degeneracy, which is given by a simple arithmetic average over the two e_g states. Thus the electron configuration at two Mn^{3+} ($3d^4$) cations separated by an anion intermediary is, for alternative (b), correlated with the nuclear motions as indicated schematically in Fig. 10, whereas for alternative (c) the electron configuration corresponds to a half-electron per e_g orbital.

From Fig. 10 it is apparent that the vibrational mode of principal interest represents the vibration of the cation and anion sublattices against one another. The frequency of this mode is the *Restrahl* frequency. Restrahl wavelengths[25] are $\approx 10^{-2}$ cm, corresponding to $h\nu_n \approx 100$ cm^{-1}. In the perovskite $LaMnO_3$, the O'-orthorhombic $\rightleftharpoons$ rhombohedral transition[26] occurs at about 900°K, and in the spinel Mn_3O_4 a tetragonal $\rightleftharpoons$ cubic transition[27] occurs at about 1443°K. The fact that the cooperative transition temperature varies with the number of Mn^{3+} ions that are present indicates that the Jahn-Teller stabilization per Mn^{3+} ion ΔE_{JT} can be properly estimated from the transition temperature only if all the cations present are octahedral-site Mn^{3+}. However, the transition temperatures cited provide a lower bound, so that $\Delta E_{JT} > 750$ cm^{-1}. This means that Eq. (3) applies, so that the quasistatic hypothesis of alternative (b) is to be preferred to assumption (c). This assertion is supported by the magnetic data, as is shown in Sec. IV.

IV. DISCUSSION

A. Perovskite Systems

Perovskite-type oxides and fluorides (ABO_3 or ABF_3) are especially suited to the study of 180° cation-anion-cation magnetic interactions. Ideally the cations form a CsCl-type sublattice with anions on the edges of the simple-cubic array of B ions.[28] If the A cations are nonmagnetic, a magnetic B cation can interact magnetically (dipole-dipole interactions neglected) only with its six nearest-neighbor B cations via 180° cation-anion-cation linkages.

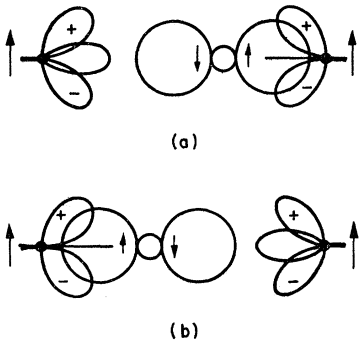

FIG. 10. Schematic diagram for quasistatic electronic order about $3d^4$ cations for two different relative positions of anion and cation sublattices. Each configuration corresponds to case 3, moderate ferromagnetism.

1. *Anisotropic Mn^{3+}—O^{2-}—Mn^{3+} Interactions*

A neutron-diffraction study[29] of $LaMnO_3$ has revealed that in this O'-orthorhombic perovskite the Mn^{3+}—O^{2-}—Mn^{3+} interactions are anisotropic, being ferromagnetic in the (001) planes and antiferromagnetic along the c axis. This anisotropic coupling was shown[1] to be compatible with the rules of Fig. 9, provided electronic ordering of the single e_g electron had been induced by a cooperative Jahn-Teller distortion of the B-ion interstices. In that original paper the ordered arrangement was assumed to be that of the high-vibration-anisotropy limit shown in Fig. 8. Subsequently Kanamori[18] showed that the ratio Q_3/Q_2 that is present in a given static distortion is given by

$$\tan\phi = \frac{(2/\sqrt{6})(2m-l-s)}{\pm(2/\sqrt{2})(l-s)}, \tag{5}$$

where s and l are the short and long cation-anion bond lengths that alternate along [100] and [010] axes, m is the bond length along [001], $s \leq m < l$, and ϕ is the angle between the state vectors and the Q_2 axis. In the high-anisotropy limit, $m=s$ and $\phi=30°$, which corresponds to $\theta = \pm 2\pi/3$. [See discussion in connection with Eq. (1).] In either the low-anisotropy limit (only $\pm Q_2$) or the high-anisotropy limit (only Q_3 with $\theta = \pm 2\pi/3$), magnetic coupling within the (001) planes is *ferromagnetic* via case 3 of Fig. 9, and along the [001] it is *antiferromagnetic* either via case 2 of Fig. 9 (high-anisotropy limit) or via a weakened case 1. Therefore measurements of the magnetic order cannot distinguish

[24] M. Born and R. J. Oppenheimer, Ann. Physik **84**, 457 (1927).
[25] C. Kittel, *Introduction to Solid-State Physics* (John Wiley & Sons, Inc., New York, 1957), 2nd ed., p. 114.
[26] A. Wold and R. J. Arnott, J. Phys. Chem. Solids **9**, 176 (1959).
[27] H. F. McMurdie and E. Golovato, J. Research Natl. Bur. Standards **41**, 589 (1948).
[28] The ideal cubic phase is rarely found in the oxides and fluorides. The influence of ionic size on the density of packing induces small distortions to orthorhombic or rhombohedral symmetry. Electronic order may induce additional distortions to be superposed on those due to ionic size (see reference 1).
[29] E. O. Wollan and W. C. Koehler, Phys. Rev. **100**, 545 (1955).

between these limits. However, careful x-ray determinations of m, l, and s can give this information via Eq. (5). Although such measurements have not been made on $LaMnO_3$ itself, such measurements have been made[30] on MnF_3, whose ideal structure is similar to perovskite with the A cations missing. It is found that $\phi(MnF_3) = 6° 35'$, which corresponds to only a modest vibrational anisotropy. Anisotropic $3d^4$-anion-$3d^4$ magnetic interactions have been directly confirmed by neutron diffraction for monoclinic MnF_3,[31] and tetragonal ($c/a<1$) $KCrF_3$,[32] where the electronic ordering at the $3d^4$ cation is manifestly similar to that found in $LaMnO_3$. These anisotropic magnetic interactions are a dramatic confirmation of the rules of Fig. 9. Further, the available x-ray data argue against the Wojtowicz assumption of high vibrational anisotropy.

2. *Isotropic $Mn^{3+}-O^{2-}-Mn^{3+}$ Interactions*

It follows from Fig. 9 that, if it were possible to obtain rocksalt-type order among two types of magnetic B cation, one with no outer e_g electrons and the other with two outer e_g electrons, ferromagnetic coupling should occur. Previous attempts to order $La(Fe_{0.5}^{3+}Cr_{0.5}^{3+})O_3$ were unsuccessful.[33] With no charge difference between the two types of B ions, there were no electrostatic forces to favor the ordered arrangement. Therefore an attempt was made to obtain ordered $La(Ni_{0.5}^{2+}Mn_{0.5}^{4+})O_3$ and $La(Co_{0.5}^{2+}Mn_{0.5}^{4+})O_3$. However, it was found[34] that the cations favor $La(Ni_{0.5}^{III}Mn_{0.5}^{3+})O_3$ and $La(Co_{0.5}^{III}Mn_{0.5}^{3+})O_3$, so that again there were no electrostatic forces to induce ordering on the B sublattice.[35] However, the systems $La(Co,Mn)O_3$ and $La(Ni,Mn)O_3$ provide an opportunity to study the important $Mn^{3+}-O^{2-}-Mn^{3+}$ interactions.

Previous paramagnetic-susceptibility measurements by Jonker[36] have suggested that antiferromagnetic $LaMnO_3$ has only ferromagnetic $Mn^{3+}-O^{2-}-Mn^{3+}$ interactions at high temperatures. Jonker also reported that samples of $La(Mn_{1-x}Al_x)O_3$, $x<0.5$, were nonmagnetic, whereas the system La^{3+}, $Ba^{2+}(Mn^{3+},Ti^{4+})O_3$ is "ferromagnetic." To help resolve these apparently conflicting results, samples in the $La(Mn,Ga)O_3$ system were also prepared for the study of $Mn^{3+}-O^{2-}-Mn^{3+}$ interactions.

At high temperatures and/or with sufficient dilution of the B-cation sublattice with non-Jahn-Teller ions, there is no static, cooperative distortion of the structure that reflects electron ordering at the Mn^{3+} ions. It was pointed out that there are three possible assumptions; (a) random, static distortions, (b) the quasistatic hypothesis, and (c) no static distortions and no correlation between neighboring electron configurations. For alternative (a), the $Mn^{3+}-O^{2-}-Mn^{3+}$ interactions are randomly case 1, case 2, or case 3 of Fig. 9. Such a model would predict no long-range magnetic order and the possibility of a ferrimagnetic moment. For alternative (b), the electron configurations of neighboring Mn^{3+} ions are correlated as shown in Fig. 10, so that the magnetic coupling is ferromagnetic, corresponding to case 3 of Fig. 9. For alternative (c), the e_g orbitals, which have a twofold spin degeneracy, are quarter-filled, and the superexchange mechanisms dictate that in such a case rules for the sign of the interaction are those for half-filled e_g orbitals. Therefore with alternative (c), antiferromagnetic $Mn^{3+}-O^{2-}-Mn^{3+}$ interactions are predicted.

Trivalent cobalt is often found to be diamagnetic when located in an octahedral interstice of an O^{2-} sublattice.[37,38] Although paramagnetic $LaCoO_3$ contains[39] high-spin-state Co^{3+}, which presumably couples antiferromagnetically according to case 1 of Fig. 9, trivalent cobalt appears to be in its low-spin state in $La(Mn_{1-x}Co_x)O_{3+\delta}$, at least for $x\leq 0.5$. For larger values of x, there may be a mixture of low-spin and high-spin trivalent cobalt.[40] In this discussion, it is assumed that the crystalline fields are sufficiently large to render trivalent cobalt diamagnetic, $Co^{III}(t_{2g}^6e_g^0)$ for $x\leq 0.5$. Similarly trivalent nickel is assumed to be in its low-spin state, $Ni^{III}(t_{2g}^6e_g^1)$.

It is significant, therefore, that O-orthorhombic $La(Mn_{1-x}Co_x)O_{3+\delta}$ is ferromagnetic with a magnetization approximately $4\mu_B$/Mn atom throughout the region $0.25\leq x\leq 0.5$ (see Fig. 2). Diamagnetic cobalt cannot contribute directly to the magnetic coupling. However, by destroying the O' symmetry it destroys the cooperative, static Jahn-Teller ordering of $LaMnO_3$. Of the three alternative models for the electron configurations at the Jahn-Teller ions, only the quasistatic hypothesis [alternative (b)] is compatible with the magnetization data. It should also be noted that this conclusion is also compatible with Jonker's finding of ferromagnetic coupling in high-temperature (or rhombohedral) $LaMnO_3$ and in the system $La_{1-x}Ba_x(Mn_{1-x}Ti_x)O_3$.[41]

---

[30] M. A. Hepworth and K. H. Jack, Acta Cryst. **10**, 345 (1957).
[31] E. O. Wollan, H. R. Child, W. C. Koehler, and M. K. Wilkinson, Phys. Rev. **112**, 1132 (1959).
[32] V. Scatturin, L. Corliss, N. Elliott, and J. Hastings, Acta Cryst. **14**, 19 (1961).
[33] A. Wold and W. J. Croft, J. Phys. Chem. **63**, 447 (1959).
[34] A. Wold, R. J. Arnott, and J. B. Goodenough, J. Appl. Phys. **29**, 387 (1958).
[35] Roman-numeral valences refer to low-spin-state cations. This situation occurs if the crystal-field splitting Δ is greater than the exchange splitting E_{ex}. (See Fig. 6.) Thus Ni^{III} has the outer-electron configuration $t_{2g}^6e_g^1$, with only one unpaired spin, and Co^{III} ($t_{2g}^6e_g^0$) is diamagnetic.
[36] G. H. Jonker, Physica **22**, 707 (1956).
[37] P. Cossee, Rec. trav. chim. **75**, 1089 (1956).
[38] J. B. Goodenough, J. Phys. Chem. Solids **6**, 287 (1958).
[39] G. H. Jonker and J. H. Van Santen, Physica **19**, 120 (1953).
[40] Such a mixture could conceivably be reflected in the two magnetic (and crystallographic) phases that were observed in the sample with $x=0.5$. A phase containing high-spin-state Co^{3+} would have a higher Curie temperature than one containing diamagnetic Co^{III}.
[41] This system approaches but does not attain a magnetization of $4\mu_B$/Mn atom. The magnetization is sufficiently high that ferrimagnetism via alternative (a) seems less probable than ferrimagnetism due to chemical inhomogeneities in the sample.

3. *The System* $La(Mn_{1-x}Ga_x)O_3$

In our study of the system $La(Mn_{1-x}Ga_x)O_3$, it was found that the O'-orthorhombic phase persists up to $x=0.5$. $LaGaO_3$ is rhombohedral above 900°C, O-orthorhombic at room temperature,[42] so that size effects favor the orthorhombic phase. If the introduction of diamagnetic Ga^{3+} into the O'-orthorhombic phase caused the $Mn^{3+}-O^{2-}-Mn^{3+}$ interactions to become isotropic and ferromagnetic, as in the case of similar concentrations of diamagnetic Co^{III} and Ti^{4+} in the O-orthorhombic phase, then the magnetization curve for the system $LaMn_{1-x}Ga_xO_3$ would be similar to that for $LaMn_{1-x}Co_xO_{3+\delta}$. The fact that this is not the case (compare Figs. 1 and 2) argues strongly that the crystallographic symmetry does indeed reflect electron ordering that permits anisotropic $Mn^{3+}-O^{2-}-Mn^{3+}$ coupling.

However, if Ga^{3+} were to enter the Mn^{3+} sublattice randomly, but without destroying the static Jahn-Teller ordering responsible for the O' symmetry, the system $La(Mn_{1-x}Ga_x)O_3$ would remain antiferromagnetic, the only change in the electronic ordering about a Mn^{3+} cation having a Ga^{3+} neighbor being an adjustment of the electron concentrations between the m and l bonds. In fact this is the result that was anticipated, since we suspect that Jonker's $La(Mn_{1-x}Al_x)O_3$ samples were probably of O' symmetry with Al^{3+} substituted *randomly* for Mn^{3+}. It is obvious from Fig. 1 that the O' phase is not antiferromagnetic in the range $0<x<0.5$. However a straightforward interpretation of the magnetization data of Fig. 1 is available if the Ga^{3+} order preferentially into alternate (001) planes when $x<0.5$. This assumption is made in the following discussion of the data even though a direct observation of atomic ordering has not been made. The theoretical plausibility of this assumption is discussed subsequently.

Given O' symmetry, the static electron ordering at the Mn^{3+} ions remains essentially the same as in O' $LaMnO_3$, so that the rules of Fig. 9 call for ferromagnetic (001) planes coupled antiparallel to one another. With preferential ordering of Ga^{3+} into alternate (001) planes, there must be a spontaneous magnetization per molecule μ_s. For perfect order,

$$\mu_s=4x\mu_B, \quad x<0.5. \tag{6}$$

In Fig. 1 this prediction is compared with the experimental points. Further, for $x>0.5$, where the symmetry is O-orthorhombic, ferromagnetism via the quasistatic mechanism is predicted, or

$$\mu_s=4(1-x)\mu_B, \quad x>0.5. \tag{7}$$

This line is also shown in Fig. 1.

Agreement between theory and experiment is quite satisfactory in the range $0<x<0.4$. In the range $0.6\leq x\leq 1.0$ there is sufficient dilution of the Mn^{3+} sublattice by Ga^{3+} that not all of the Mn^{3+} can be cooperatively coupled. Therefore agreement between theory and experiment is quite satisfactory in this range also. In the intermediate range $0.4<x<0.6$, chemical inhomogeneities can be expected to be important so that Ga^{3+} ordering is not complete and domains of O-orthorhombic material could be present within the O'-orthorhombic phase or O' material within the O phase, without detection by the x-ray patterns. Throughout this range, the diffraction lines are considerably broadened, which is compatible with a heterogeneous mixture of static and dynamic Jahn-Teller effects at the Mn^{3+} ions.

Further evidence for Ga^{3+} ordering is given by the Curie-point data. With no change in the magnetic-coupling mechanisms within the O' phase, introduction of Ga^{3+} into alternate (001) planes would depress the Curie point at a rate that would make it approach 0°K at $x=0.5$.[43] Such a depression of T_c is found in the range $0<x<0.4$. Deviations to higher T_c in the range $0.4<x<0.6$, but no sharp discontinuity at $x=0.5$, is compatible with a gradual breakdown of Ga^{3+} ordering and two orthorhombic phases throughout this region. The Curie temperature for disordered material would be higher than that for ordered material because of the greater number of Mn^{3+} links between Mn^{3+}-rich (001) planes. That there should be a higher T_c for ferromagnetic O-orthorhombic domains, in which the magnetic-coupling mechanisms are changed, is evident from the Curie temperatures found in O-orthorhombic $La(Mn_{0.75}Co_{0.25})O_{3+\delta}$ and $La(Mn_{0.5}Co_{0.5})O_{3+\delta}$, which are also shown in Fig. 1. With fine-grained chemical inhomogeneities responsible for the two phases, the two phases would be magnetically coupled so as to render but a single T_c. This type of magnetic coupling between ferromagnetic and ferrimagnetic or antiferromagnetic domains to give a single T_c is characteristic of those materials that exhibit exchange anisotropy.[44]

It is concluded, therefore, that the magnetic data for the system $La(Mn_{1-x}Ga_x)O_3$ strongly implies Ga^{3+} ordering into alternate (001) planes for $0<x<0.4$ and a breakdown of this ordering in the range $0.4<x<0.6$. Lack of such order would imply that the electron configurations at the Mn^{3+} ions of the O'-orthorhombic phase changes in a complicated manner that depends upon the number of Ga^{3+} neighbors.

Since there is no charge differential between the Mn^{3+} and Ga^{3+} ions, it is important to enquire how ordering is possible in the $La(Mn,Ga)O_3$ system when it is not found in other $La(Mn,M^{3+})O_3$ systems. Although we have no definitive answer to this problem, it is possible that the elastic energy associated with the static electron ordering of the O' symmetry is optimized by atomic ordering. The opposite motions of the O^{2-} ions in

[42] S. Geller, Acta Cryst. **10**, 161 (1957).

[43] With perfect ordering at $x=0.5$, the Mn^{3+} (001) planes are sufficiently isolated from one another that the interplanar coupling must be extremely weak (<30°K).

[44] W. H. Meiklejohn and C. P. Bean, Phys. Rev. **102**, 1413 (1956); **105**, 904 (1957).

alternate (001) planes (see Fig. 8) show that alternate (001) planes are differentiated elastically. However this mechanism requires O' symmetry at temperatures that are sufficiently high for atomic mobility. This requirement is barely fulfilled in $LaMnO_3$, where the $O' \rightleftharpoons R$ transition temperature is $T_t \approx 900°K$. However T_t must decrease with increasing x, and for x greater than some critical composition x_c, the atomic mobility for $T < T_t$ is too low for appreciable ordering to take place. Such a mechanism is compatible with the fact that Ga^{3+} ordering appears to break up in the region $0.4 < x < 0.5$ even though the ordering energy is presumably greatest at $x = 0.5$.

4. *The System $La(Mn_{1-x}Ni_x)O_{3+\delta'}$*

The cation $Ni^{III}(t_{2g}^6 e_g^1)$ should also be a Jahn-Teller ion. Therefore in an O-orthorhombic or a rhombohedral phase, all interactions ($Mn^{3+}-O^{2-}-Mn^{3+}$, $Mn^{3+}-O^{2-}-Ni^{III}$, and $Ni^{III}-O^{2-}-Ni^{III}$) should be ferromagnetic, according to the quasistatic hypothesis. This appears to be fulfilled in $La(Mn_{1-x}Ni_x)O_{3+\delta'}$ for $x < 0.5$ (see Fig. 3). (By contrast, the other alternatives are only compatible with either antiferromagnetic coupling or a weak ferrimagnetism.) For $0.5 \leq x \leq 1.0$, there is a two-phase region in which some La_2NiO_4, with K_2NiF_4 structure, is present. However, rhombohedral $LaNiO_3$ has no spontaneous magnetization, and there is no evidence of magnetic order[45] down to 4.2°K. This indicates that although the $Mn^{3+}-O^{2-}-Ni^{III}$ interactions are ferromagnetic as anticipated, there is no superexchange coupling between Ni^{III} cations. Actually it is not unreasonable that this breakdown of superexchange coupling should occur for interactions between cations with total spin $S = \frac{1}{2}$, since the two principal superexchange mechanisms assume that in the excited states that are admixed to the ground state to give the magnetic coupling, the excited-electron spins remain correlated with the net spins on the two cations. For the case $S = \frac{1}{2}$, there is no net cation spin with which the "excited" electron can remain correlated, since the excited states are singlets with zero net spin at each cation. That the lack of ferromagnetism in $LaNiO_3$ is due to a breakdown of the superexchange mechanism between cations with $S = \frac{1}{2}$ and not to a breakdown of the quasistatic hypothesis, is supported by the observation that RuF_3 and PdF_3, like $LaNiO_3$, exhibit no magnetic order[46] above 4°K. The structure of these fluorides is like perovskite with the A cation missing, and Ru^{III} and Pd^{III} are both spin-quenched by the ligand fields so that $S = \frac{1}{2}$.

5. *Interactions between Jahn-Teller and Non-Jahn-Teller Ions*

If cation M is not a Jahn-Teller ion, there is no coupling of its outer-electron configuration with the vibrational modes. Therefore there can be no dynamic correlation of electron configurations at a Jahn-Teller ion like Mn^{3+} with those at a neighboring M atom. This means that if there are no static distortions at the Mn^{3+}, local or cooperative, the Mn^{3+} interacts isotropically as though its e_g orbitals were half-filled.[47]

That this prediction is in agreement with experiment is demonstrated by the ferromagnetic $Mn^{3+}-O^{2-}-Mn^{4+}$, $Mn^{3+}-O^{2-}-Cr^{3+}$ interactions, the antiferromagnetic $Cr^{3+}-O^{2-}-Cr^{3+}$, $Mn^{4+}-O^{2-}-Mn^{4+}$, $Mn^{3+}-O^{2-}-Fe^{3+}$, and $Fe^{3+}-O^{2-}-Fe^{3+}$ interactions that have been observed in the $La(Mn,Cr)O_3$, $La(Mn,Fe)O_3$, and $(La,Co)MnO_3$ systems.[33,36,45,48,49] The $Ni^{III}-O^{2-}-Ni^{2+}$ interactions in $Li_xNi_{1-x}O_2$ also appear to be antiferromagnetic.[50]

6. *Conclusion*

With the aid of the quasistatic hypothesis, it is possible to predict all the varied 180° superexchange interactions of a $3d^4$ cation. In Table I this is done for perovskite-type compounds.

B. Implications for NiAs Systems

It is an interesting fact that all of the ferromagnetic NiAs-type materials contain, formally at least, $3d^4$ cations: $Cr_{1+x}Te$ ($2.4\mu_B$/Cr),[51] MnAs, MnSb, MnBi: (3.4–$3.5\mu_B$/Mn^{3+}).[52] Well-annealed MnBi approaches[53,54] $3.95\mu_B$/Mn^{3+}. (The compound $\gamma Fe_{1.3}Sn$ ($2.3\mu_B$/Fe)[55] is undoubtedly ferrimagnetic, the sublattice of interstitial iron ions coupling to the sublattice of octahedral-site iron ions.) In each of these compounds there should be a relatively strong, antiferromagnetic cation-cation (no anion intermediary) interaction along the hexagonal c axis since cation-occupied octahedra share a common face, thus permitting considerable overlap of their half-filled t_{2g} orbitals.[56] Hence it is not surprising that ferromagnetism is only found with large anions, the stability increasing with larger ratio of intercation distance to cation diameter. Therefore ferromagnetism and the possibility of "exchange-inversion" magnetization,[57] recently discussed by Kittel,[58] are only understandable provided a competitive, ferromagnetic exchange mechanism is available.[59]

---

[45] W. C. Koehler and E. O. Wollan, J. Phys. Chem. Solids **2**, 100 (1957).

[46] M. K. Wilkinson, E. O. Wollan, H. R. Child, and J. W. Cable, Phys. Rev. **121**, 74 (1961).

[47] This corresponds to alternative (c).

[48] U. H. Bents, Phys. Rev. **106**, 225 (1957).

[49] M. A. Gilleo, Acta Cryst. **10**, 161 (1957).

[50] J. B. Goodenough, D. G. Wickham, and W. J. Croft, J. Phys. Chem. Solids **5**, 107 (1958).

[51] C. Guillaud and S. Barbezat, Compt. rend. **222**, 386 (1946).

[52] C. Guillaud, J. phys. radium **12**, 223 (1951).

[53] R. R. Heikes, Phys. Rev. **99**, 446 (1955).

[54] B. W. Roberts, Phys. Rev. **104**, 607 (1956); J. Metals **8**, 1407 (1951).

[55] M. Asanuma, J. Phys. Soc. Japan **15**, 1343 (1960).

[56] J. B. Goodenough, Phys. Rev. **117**, 1442 (1960).

[57] T. J. Swoboda, W. H. Cloud, T. A. Bither, M. S. Sadler, and H. S. Jarrett, Phys. Rev. Letters **4**, 509 (1960).

[58] C. Kittel, Phys. Rev. **120**, 335 (1960).

[59] In MnAs and MnBi the χ vs T curves indicate two magnetic transitions. Neutron diffraction (reference 54) reveals no evidence

Since cooperative, static Jahn-Teller distortions are not found in the NiAs structure (with the exception of antiferromagnetic CrS),[60] a possible mechanism for the competitive, ferromagnetic exchange is $3d^4$-anion-$3d^4$ superexchange with quasistatic correlations. If this is the mechanism, the NiAs compounds are essentially ionic and their metallic conductivity is due to cation-sublattice d-band formation that is made possible by the presence of a large number of interstitial cations.[61]

Another alternative, it must be noted, is that the cation $3d$ levels, which for ionic compounds lie in the energy gap between the filled, bonding and the empty, antibonding $s-p$ states, fall sufficiently near the top of the energy gap, which is reduced in less ionic materials, so that the less stable e_g states mix with the antibonding $s-p$ states. Antibonding electrons can be expected[62] both to couple the localized t_{2g} electrons ferromagnetically and to provide metallic conductivity. A study of electron mobilities should be able to differentiate between these alternative mechanisms for ferromagnetic coupling between the $3d^4$ cations of NiAs-type compounds.

ACKNOWLEDGMENT

The authors would like to acknowledge the assistance of R. W. Germann who helped prepare several of the compounds.

APPENDIX

1. Delocalization Superexchange

The delocalization mechanism consists of a drift of one electron from one cation to the other, the transfer integral b_{ij} for the process varying as the square of the overlap of cation and anion orbitals since partial covalency of the anion-cation bond forces the cation d orbitals to spread out over the anion. The analytic expression, which comes from second-order perturbation theory, gives a magnetic-coupling energy proportional to b_{ij}^2/U, where U is the energy required for the electron transfer. All the important contributions to the superexchange show this fourth-order dependence on the overlap of nonorthogonal cation and anion orbitals.

The rules for the sign of the interaction follow from the fact that the transfer integrals carry an electron without change of spin. Case 1 of Fig. 9 represents transfer between half-filled, cation $\sigma(e_g)$ orbitals. Since the Pauli exclusion principle limits a given orbital to one electron of each spin, this means that the interacting electrons must be antiparallel if transfer is to take place. If the cation $\pi(t_{2g})$ orbitals are also half-filled, these also contribute some antiferromagnetic superexchange. In case 2 of Fig. 9, only the π-bond interaction is present, and weak antiferromagnetism results. Case 3 corresponds to superexchange between an empty and a half-filled $\sigma(e_g)$ orbital. In this case the transferred electron may, compatible with the Pauli principle, have either spin. However if the transferred electron is parallel to the net spin of the recipient cation, it is stabilized, relative to an antiparallel electron, by intra-atomic exchange J_{intra}. Therefore the σ-bond superexchange is ferromagnetic; but it is weaker than Case 1 σ-bond superexchange by the factor J_{intra}/U. Although antiferromagnetic π bonding may be simultaneously present, it is found experimentally that the weakened σ-bond coupling predominates. It may therefore be considered of moderate relative strength.

2. Correlation Superexchange

The correlation mechanism takes into account the *simultaneous* partial-bond formation on either side of the anion. The cation spins are so coupled that the two anion $p\sigma$ electrons, one of each spin, can simultaneously form partial-covalent bonds on opposite sides of the anion. The rules for the sign of the interaction follow immediately from the schematic diagrams of Fig. 9. Spin

TABLE I. Predicted $(3d^4)$—anion—M interactions.

n[a]	M[b]	O' symmetry[c] In (001) plane	O' symmetry[c] Along [001] axis	O or R symmetry[d] All directions
0	Ti^{3+}, Zr^{3+}, Ru^{6+}, V^{3+}, Nb^{3+}, Os^{6+}, Cr^{3+}, Mo^{3+}, Mn^{4+}, Ir^{6+}	Cases 3 and 2	Case 2 (or 3)	Case 3
1	Cr^{2+}, Mn^{3+}, Fe^{4+}, Ni^{III}	Case 3	Case 2 (or 1)	Case 3
2	Mn^{2+}, Fe^{3+}; Fe^{2+}, Co^{3+}, Co^{2+}, Ni^{3+}; Ni^{2+}, Au^{3+}	Cases 1 and 3	Case 3	Case 1
3	Cu^{2+}	None	Case 1 or none	Weak Case 1

[a] n = number of e_g electrons.
[b] Arabic valence refers to high-spin state, roman numerals to low-spin state.
[c] Illustrative of static electronic order at $3d^4$ cations.
[d] Illustrative of crystalline symmetry that does not induce static splitting of E_g state.

for long-range antiferromagnetic order below the higher temperature transition. Below the lower temperature transition the material is ferromagnetic. It is suggested that the high-temperature transition represents short-range antiferromagnetic coupling between interstitial and cation-sublattice manganese ions. The interstitials would then account for the reduced ferromagnetic moment of $3.5\mu_B$/Mn, as against $4.0\mu_B$/Mn predicted from spin-only theory and the high-temperature Curie constant.

[60] F. Jellinek, Acta Cryst. **10**, 620 (1957).

[61] NiAs compounds are difficult to define experimentally because of the availability of the interstitial sites. Because tetrahedral interstices of the close-packed anion sublattice share a common face, they combine to form a trigonal bipyramid. Occupancy of the bipyramid favors $c/a \approx 1.21$ whereas close packing favors $c/a \approx 1.63$. Observed axial ratios are frequently $c/a \approx 1.4$. Interstitial sites share a common face with the octahedral sites, so that cation-cation separations small enough for the formation of collective-electron bands may be achieved via interstitial cations even if this is not possible without the presence of interstitial cations. The e_g electrons that would be responsible for quasistatic, ferromagnetic coupling do not participate in the collective-electron bands.

[62] J. B. Goodenough, Phys. Rev. **120**, 67 (1960).

correlations within σ bonds involving empty e_g orbitals are reduced by the factor J_{intra}/U' to give the relative strengths indicated.

3. Polarization Superexchange

The polarization mechanism consists of an induced spin polarization of a doubly occupied core orbital by admixture of an unoccupied atomic valence orbital. Keffer and Oguchi[10] used nonorthogonal orbitals and obtained a sizeable effect since some delocalization and correlation superexchange were thereby included. If orthogonal orbitals are used throughout, the various polarization mechanisms[9,10] turn out to be inconsistent with the form of Eq. (2), but considerably smaller than the correlation and delocalization superexchange.[22]

PHYSICAL REVIEW VOLUME 124, NUMBER 2 OCTOBER 15, 1961

3d Band Structure of Cr

M. ASDENTE
Laboratori CISE, Milano, Politecnico di Milano, Milan, Italy

AND

J. FRIEDEL
Physique des Solides, Faculté des Sciences, Orsay (Seine et Oise), France

(Received April 26, 1961)

The electronic structure of the 3d band in Cr is calculated in the tight-binding approximation; the effect of the nearest-neighbor interaction and of the second-nearest-neighbor interaction on the energy surfaces in the Brillouin zone and on the density-of-states curve $g(E)$ is investigated.

By means of group theory, an analysis of the electron levels and of the eigenfunctions is performed in some particular points of the Brillouin zones; bonding and antibonding characters are found, together with different space distributions, for the eigenfunctions at the bottom and at the top of the band.

A comparison with other theoretical results suggests that the details of the chosen potential do not influence the general trend of the $g(E)$ curve very much; also satisfactory is a comparison with experimental results (particularly concerning electronic specific heat C_v, magnetic susceptibility χ, and thermoelectric power).

INTRODUCTION

THE central problems concerning transition metals are the determination of energy level distribution, the knowledge of the related wave functions, and the space density of charge. The properties observed along the three series of transition metals, particularly the electronic specific heat C_v and the magnetic susceptibility χ, suggest a high density of states at the Fermi level for most of them and the presence of some peaks in the density-of-states curve $g(E)$ as a function of energy. Theoretically, a self-consistent solution of the problem is prohibitively hard; a number of approximations must be made to make the problem manageable and one cannot always foresee exactly how much uncertainty each approximation introduces.

Nevertheless some results obtained so far by different methods[1–3] are satisfactory at least qualitatively and a preliminary calculation also, even with drastic approximations, permitted Slater and Koster[4] to expect a minimum at the middle of the density-of-states curve for the bcc, as the low values of C_v and χ for Cr, Mo, and W suggest.

[1] G. C. Fletcher and E. P. Wohlfarth, Phil. Mag. **42**, 106 (1951).
[2] E. F. Belding, Phil. Mag. **4**, 1145 (1959).
[3] J. H. Wood, Phys. Rev. **117**, 714 (1960).
[4] J. C. Slater and G. F. Koster, Phys. Rev. **94**, 1498 (1954).

In this paper a calculation on the structure of the 3d band in Cr is made using the tight-binding approximation. The present calculation was performed to see the effect of the nearest- and second-nearest-neighbor interactions on the energy surfaces in the Brillouin zone and on the $g(E)$ curve, to investigate further, by comparison to the results of others, the influence of potential choice, and other comparisons of interest to both previous calculations and experimental results. Also, an analysis is given of the information that can be deduced by group theory about the electron levels and the eigenfunctions.

CALCULATION OF $E(k)$ CURVES

A series of Bloch functions $\Phi_n(\mathbf{r},\mathbf{k})$ is built up starting from the five $f_n(\mathbf{r})$ normalized functions corresponding to the fivefold-degenerate 3d level of a single atom:

$$f_1=\frac{1}{N_1}xyf(r),\quad f_2=\frac{1}{N_1}yzf(r),\quad f_3=\frac{1}{N_1}zxf(r),$$

$$f_4=\frac{1}{N_2}(x^2-y^2)f(r),\quad f_5=\frac{1}{N_3}(3z^2-r^2)f(r),\quad (1)$$

$$\Phi_n(\mathbf{r},\mathbf{k})=\sum_1 \exp(i\mathbf{k}\cdot\mathbf{R}_1)f_n(\mathbf{r}-\mathbf{R}_1),\quad n=1,2,3,4,5,\quad (2)$$